集束イオンビームによりナノ加工を施した $LiNbO_3$ フォトニックデバイス

Nano-fabrication of $LiNbO_3$ by focused ion beam for novel photonic devices

李 西 軍，渡 辺 温
Li Xijun, Watanabe Atsushi

要　旨　ナノ加工技術の進歩により、斬新で高性能な光デバイスの研究開発が益々盛んになってきている。シリコン・オン・インシュレータ（ＳＯＩ）分野ではすでに成熟しているナノリソグラフィやナノエッチングなどのトップダウン型のナノ加工技術を駆使し，スラブ型フォトニック結晶やフォトニック・ワイヤーなどが次々と報告されている。我々は，集束イオンビーム（ＦＩＢ）を用いることにより，まだ未成熟分野であるシリカ上ニオブ酸リチウム（ＬＮ）薄膜に対するナノ加工技術を確立し，フォトニック結晶構造の作製に成功した。さらにＬＮのリッジ型導波路において，ＦＩＢによるサブミクロン・オーダーの直接ドメイン・パターニングも達成することができた。最後に集積型ＬＮ非線形光デバイスと高集積光回路ＬＮフォトニック結晶に言及する。

Abstract:　Novel and high performance photonic devices benefited from nanofabrication attract more and more research interests. By applying already matured top-down nanofabrication techniques for silicon on insulator (SOI), photonic crystal slabs[(1)] and photonic wires[(2)] can be well fabricated. In this paper, we will report our recent progresses of applying focused ion beam (FIB) to engineering thin $LiNbO_3$ (LN) layer on silica (LNoI), for which no mature nanofabrication techniques are available. In addition to successfully fabricated photonic crystal (PhC) structures, we also succeeded in directly patterning ferroelectric domains at sub-micro scale in LN ridge waveguide. Both integrated nonlinear optical devices and highly integrated optical circuits in LN PhC are also presented.

Keywords：Lithium niobate, focused ion beam, nanofabrication, photonic device

1. Introduction

Integrated optics, a system parallel with integrated electronics (also known as microelectronics), could be a good candidate for future information technologies because optics has very broad band width, excellent resistance to electromagnetic interface and the possibility of multiplex. Not long after the invention of integrated electronic technology [(3)], integrated optics has been proposed and developed [(4)]. Unfortunately, more than 20 years after its conception, until middle 1990s, integrated optics didn't earn more for the world as its original fans expected, though semiconductor laser, low-loss optical fiber and Er-doped fiber amplifier have already been well commercialized in worldwide internet backbones. The main reason for the failure of integrated optics is the propagation properties of optical wave. To integrated optics on a single chip, individual optical component needs to be connected with each other. The mainstream of optical connection wires before middle of 1990s is low index difference ($\Delta n < 0.1$) waveguide. For such a waveguide, sharp bend of radius of several tens micrometers will give an unbearable bend loss for the guided wave. This limits the optics to be integrated only on a board, not on a chip. In fact, it is not overstated to say that there is no true integrated

optics by then.

Thanks to the improved understanding of photon-material interaction during the 1990s, scientists and engineers around the world now take the chance to explore another three types of optical-wave guiding structures to serve integrated optics as the connection wire. They are high refractive index difference (HID) waveguide, usually made of silicon [2], metal/dielectric material interface waveguide utilizing surface plasmon polaritons [5], and wave guiding using line defects in photonic crystals [6]. Because of the relatively small refractive index of $LiNbO_3$, we will omit HID waveguide in this paper and concentrate on photonic crystal based optical integration.

Benefited from the matured processing technologies of microelectronics, 2D silicon photonic crystal can be easily fabricated and many photonic crystal based devices, such as waveguide [6], nano-resonators [7], lasers [8], filters [9], sharp bends [10], add and droppers [11] have been demonstrated. To fully develop monolithic integrated optical devices for information processing, usually non-linear optical devices are needed. Silicon, however cannot satisfy such a nonlinearity requirement though recently silicon photonics has been exploited, such as silicon Raman laser [12], silicon modulators [13]. In this paper, as stated, we will concentrate on LN, which is more popular to nonlinear optics researchers than to electronic engineers. In fact, this material, LN, is not a stranger to your daily life. For example, in most of the cell phones, this material supports the transceiver function as surface acoustic wave (SAW) filter [14]. Though LN is more famous to nonlinear optical researchers, at present, the largest consumer of this material is not the nonlinear-optical component manufacturers, but the SAW application to cell phones.

This study aims at using this material for small-scale integration of the optical components by exploiting nonlinear optical property and PhC devices. Unfortunately, no matured nano-fabrication techniques now are available to this material as to silicon or III-V semiconductors. So we tried to divide our process into to two steps. The first step is parallel micro-scale structure preparation with conventional top-down processes, say photo-lithography and dry etching. The second step is to exploit FIB to be the nano-fabrication facility with an acceptable fabrication rate. In addition to conventional FIB milling techniques, we proposed and demonstrated domain-patterning ability of FIB at nanoscale, which may bring high performance quasi-phase matched nonlinear optical device into reality.

In this paper, all the LN samples are thin layers on silica. The thin single crystalline layer of 500μm thick was set on 1μm thick silica, which was sputtered on a congruent lithium niobate substrate. The LN sample was then reduced to 2-3μm thick with a mechanical and chemically polishing. Cross section of the sample is shown in Fig.1 where a 100nm thick metal layer under silica was also included. Function of this metal layer will be addressed later in this paper.

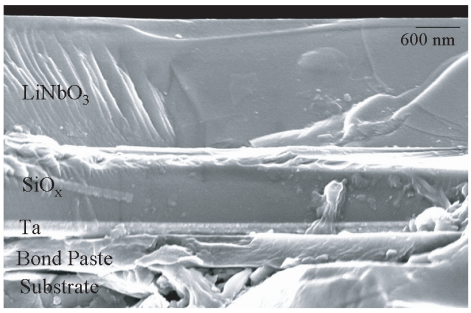

Fig.1 SEM image of cross section of LNoI.

2. Microstructure preparation

As mentioned above, because of the relatively slow process of FIB nanofabrication at large size scale, we applied silicon planar fabrication to structuring thin lithium LNoI at micro-scale. The process can be outlined in Fig.2. First, an etching mask was developed on the sample layer with photolithography method. Dry etching was then applied to transfer the mask pattern into the sample.

As the dry etching process in LN is mainly physical

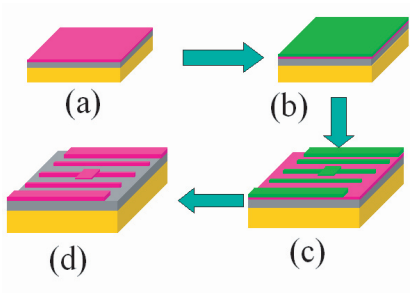

Fig.2 Schematics of LNoI micro-fabrication. LNoI (a), Mask coating (b), Mask patterned (c) and Pattern transfer to LNoI (d).

sputtering. The sidewall of the structure is tilted, not vertical, as shown in Fig.3, which shows a ridge waveguide developed in lithium niobate of 2μm thick. In addition to the tilt sidewall, the sidewall roughness is about 100nm. This roughness is not from the dry etching for pattern transition, but from the pattern mask. In order to reduce the propagation loss of light beam in the device, this sidewall roughness needs to be reduced to less than 20nm. Better mask patterning method is under investigation.

At this stage, the etching rate of LN is around 70nm per minute and the tilt angle is around 75 degree. These etching parameters are enough for fabrication structured LNoI device at micrometer scale for fabrication at nanoscale as described in the following sections.

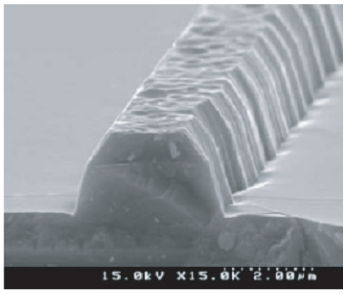

Fig.3 Cross section of an etched ridge shape structure

3. Photonic crystals and its applications

Photonic crystal is a new research field that originated in the paper of photonic band formation in early 1990s. According to the past 20 years' research progress, PhC based device gives promise to high-density photonic integrated circuits. Many novel photonic devices at very small sizes have been demonstrated [(6) ~ (11)]. In the PhCs, light beam suffers a high-low refractive index modulated media during its propagation through the crystal as electron does suffer a potential modulation in a semiconductor, thus there forms a PhC band structure for the propagating light wave. In the band gap, light propagation in this refractive index modulated media is forbidden. The originally transparent material can be blind to optical beam by structuring. Additionally, if structure defects are introduced to the so-called PhCs, defect mode can be introduced into the so-called photonic band gap. This means that forbidden wavelength in a pure PhC can thus be possible to propagate in the crystal again along the introduced line defect. One direct device is that by introducing a line defect in the PhC, a so-called PhC waveguide can be fabricated. This new waveguide guides the light beam by mechanism of photonic band gap other than refractive index difference as used in optical fibers and other channel waveguides. The ideal propagation loss for this new type waveguide is 0. By forming photonic band, the dispersion of a light pulse in the photonic crystal can be well modified and controlled [(15)]. This property can be applied to design new dispersion device for phase compensation. Interestingly, by the dispersion modification near the so-called flat band, the group dispersion of a pulse can be much larger, say larger than 1000. This means that a pulse propagating along this waveguide has a group velocity about 1000 times smaller than that of vacuum speed of light. This effect is the so-called slow light. Making use of the slow light effect, nonlinear interaction of light with the material can be largely enhanced. This is a good way to develop ultra-small nonlinear optical devices, which are important for integrated photonic circuits for information processing and storage.

Of course there are still many new optical phenomena in PhCs, such as negative effective refractive index [(16)], which will result in an imaging resolution at sub wavelength scale, or superlens effect. Our attention in photonic crystal of LN aims at novel nonlinear optical devices and integrated nonlinear photonic circuits for information technology and then our device will focus on PhC waveguide, defect mode for high quality resonator and slow wave effect. To fabricate a photonic crystal in aforementioned micro-structured LNoI, and to make the best use of modified optical propagation in PhC for second-order nonlinear optical device or electro-optical devices, 2D PhC slab needs to be fabricated in nonlinear optical materials other than semiconductors, for example, in LN. Unfortunately, traditional semiconductor fabrication tools cannot be easily applied to fabricating this material with accuracy satisfying PhC requirements. FIB milling has been applied to fabricate PhC in a bulk LN crystal [(17)]. By using proton exchange, the authors also demonstrated the confined optical beam propagating through the PhC [(18)]. However, in this device, the refractive index (n) difference between the PhC layer and the bottom substrate is defined by proton exchange and limited to less than 0.1. This value sounds too small to be good enough for practical PhC devices.

In order to fabricate a high quality PhC, we applied FIB milling technology to a thin crystalline LN layer on silica. By utilizing the larger refractive index difference between LN (in the case of z-cut sample used in this paper, n is around 2.2) and the silica layer (n around 1.47), a quasi-2D PhC slab has been successful fabricated. Contrast to Ref. [17], a large fabrication beam current was adopted, this ensures us to fabricate 20 × 20μm^2 PhC within 5 minutes. SEM and micro-optical characterization studies indicate the high structure quality of the quasi-2D PhC slab and the formation of both photonic band gap and line defect guide mode.

SEM image of the cross section of this multilayer sample is shown in Fig.1. To reduce the surface charge-up effect during FIB milling, a 60nm thick Cr film was sputtered on the $LiNbO_3$. A Hitachi FB-2100 system has been applied to milling the Cr-covered sample. In order to make a practical PhC device, waveguides need to be fabricated and coupled to the PhC devices. Dry etching and/or mechanical dicing have been applied for such a purpose. In the experiment, a fabricating beam current as large as 1.45nA has been applied to milling a 20 × 20 μm^2 PhC with a dosage larger than 10^5μC/cm^2. With this large beam current, it only took 5 minutes to fabricate a photonic crystal. This is very fast compared to more than 1 hour used in Ref[17].

One of the 2D PhC slab fabricated is illustrated in Fig.4. The AFM image of Fig. 4(b) indicates that the fabricated trench with an exposure dosage of one-half of that for PhC area has a depth around 600 nm. Assuming that the milling depth is proportional to milling dosage, the holes of the PhC are estimated to near 1.2 μm deep. The sidewall roughness indicated by SEM of Fig. 4 (a) indicates that the sidewall roughness of the FIB fabrication is less than 10 nm.

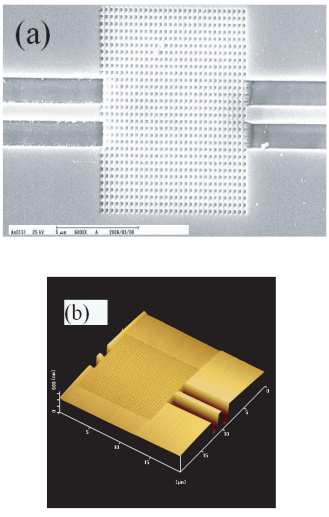

Fig. 4 LNoI Photonic Crystal Fabricated by FIB. SEM image tilted 30 degree (a) and AFM image (b).

To further confirm the milling depth of the holes in such a PhC structure, we fabricated a PhC on a square of 19 × 19 μm^2 defined by dry etching. The dry etching depth is 900nm. With the same fabricating condition of Fig. 4, the result is shown in Fig.5, which clear shows that the fabricated holes

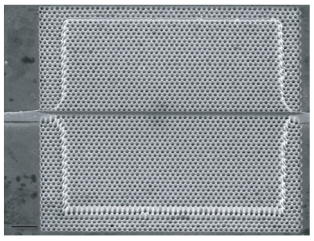

Fig.5 PhC in a dry etching defined square terrace. Scale bar is 2μm.

are much deeper than 900nm. This confirms the hole depth estimated above. Light propagation through the device is confirmed after removing the top Cr layer, as shown in Fig.6. By using a LN as thin as 1μm, a true 2D PhC slab can be fabricated by selective etching of the silica layer. The transmission spectra of both quasi-2D photonic crystal and a waveguide are listed in Fig. 6. Both photonic band gap and waveguide mode can be clearly seen. One thing needs to be addressed here is that this PhC waveguide mode seems to be higher mode other than the fundamental mode. This higher mode excitation mechanism is still under investigation. The measured result as indicated by the transmission is consistent with the simulation the calculated photonic band structure, except that band gap width of experiment is narrower than that of simulation. This may be due to the non-penetrating hole effect on this band formation.

By designing such a waveguide with flat dispersion mode, it is possible to design an electro-optical modulator as illustrated in Fig.7. For line-defect waveguide of photonic crystal, bend waveguide can be as sharp as several micrometers. With a slow light

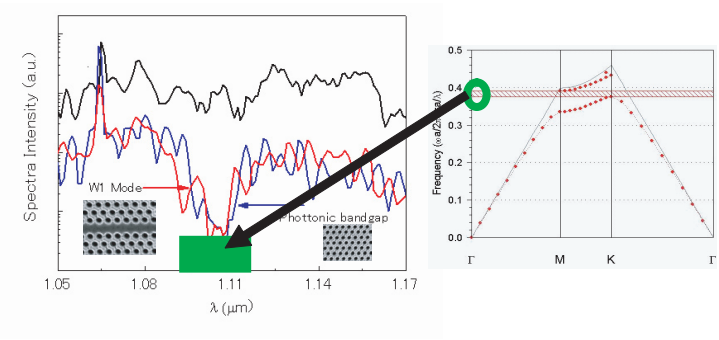

Fig. 6 Transmission spectra of PhC Slab.

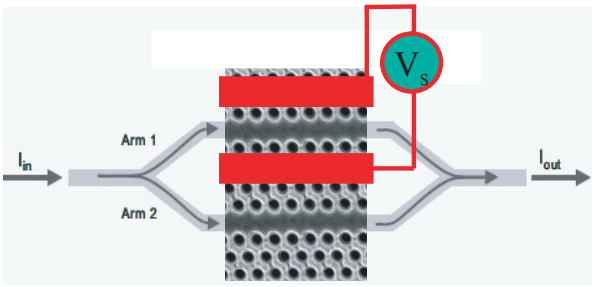

Fig. 7 PhC based EO modulator utilizing slow wave effect.

of n close to 100, the total EO modulator's length can be reduced from length of several centimeters for present channel waveguide EO modulator to less than hundred micrometers. This will largely save the LN estate and make integration at much higher density possible. Of course, there is much room for miniature of other optical devices in LN, for simplicity, we just take the EO modulator as an example here for demonstrating the future applications.

4. FIB domain engineering and QPM device

Domain patterning single crystalline ferroelectrics, such as LN and $LiTaO_3$(LT), is a critical technique to fabricate quasi-phase matched, high-efficiency wavelength conversion lasers[19]. There are many techniques to pattern ferroelectric domains in LN and LT, for example, Ti diffusion[20], electrical poling[21], and electron beam writing[22]. In order to improve the device efficiency, one can also adopt a device with highly confined optical beam within it, for example, a waveguide device to replace bulk devices. A ridge waveguide is possibly the best choice among all kinds of the waveguides [23]. For such a ridge waveguide, to obtain strong beam confinement, the active device layer is usually very thin (less than 10 μm) and has an irregular surface. Widely used electrical poling method cannot be applied to patterning domains in such a device directly because of the potential pinholes in the thin layer intrinsic to fabrication process will short the poling electrical pulses.

To fabricate such a ridge waveguide device, Ref. [23] adopted a fabrication process of patterning domain of thick layer before bonding, thinning and dicing. Among all the material family of LN, MgO doping is the best for device application because it largely improves optical damage resistance of the material against the strong beam confinement. Unfortunately, MgO doping brings difficulty to domain engineering, especially for z-cut samples that are best for device application. For example, the demonstrated domain size in a y-cut MgO:CLN is limited to a pitch size of 1.4μm[23].

In this section, we report domain patterning a z-cut MgO:CLN ridge waveguide by using domain engineering of focused ion beam (FIB)[24] ~ [27] directly. We demonstrated that FIB can engineer domains at sub-micrometer scale in a thin layer with irregular surface structures. Also we report how to improve the regularity of the fabricated domain structure by applying proper coating and the evidence of quasi-phase-matched (QPM) second harmonic generation (SHG) in such a ridge waveguide device.

The ridge waveguides used in this study were made from a thin MgO:CLN layer on silica. The cross section of the material is illustrated by SEM image of Fig.1. The thin layer was mechanical-chemically polished to 2μm thick from a z-cut MgO:CLN thick crystal slice. The thin silica serves the bottom cladding layer while a Ta layer under it as ground electrode for domain engineering. The ridge waveguide can be fabricated by using dry etching and has a width varying from 10 to 2μm and ridge height around 1μm. A Ga^{+} ion beam with proper acceleration voltage has been applied to scan on the ridge with a pitch of 100nm. The exposure dosage was controlled by both dwell time and beam current. In order to improve the quality of fabricated domain structures, a proper surface coating layer was applied to the sample. To achieve long device configuration, FIB imaging has been applied to spatially align the domains fabricated sequentially. Atomic force microscope with piezoelectric force mode and an optical characterization system have been applied to studying the domain structure in and optical properties of ridge waveguide device.

Due to the large mass of Ga+, there will be impact damages on the ridge waveguide, which potentially degrade the performance of the device. In order to protect the device from impact damage, thin protection layer has been applied.

In deed, we found that this protection layer could not only protect the ridge from impact damage but also improve the quality of the domain fabricated. Fig. 8 (a) and (b) show surface morphology and piezoelectric phase image of a domain structure with a pitch size of 7μm directly fabricated in a ridge waveguide. The stripe image of Fig. 8(a) is from the surface sputtering of Ga ion beam upon the sample surface. Due to the sputtering effect of ion beam on LN, about 20nm LN was sputtered in the beam-scanned area. The fabricated domain structure illustrated in Fig. 8 (b) is not so regular as the sputtered stripe in Fig. 8(a). To improve the domain quality and protect the ridge waveguide from sputtering, a proper layer with less surface charge-up effect should be applied. Fig. 9(a) and (b) illustrate the surface morphology and corresponding domain structure with a pitch size of 600nm fabricated in the MgO:CLN ridge waveguide coated with protection layer. After domain engineering, the protection layer was striped off for investigating the domain. It is clear from Fig. 9(a) that after striping the layer, there is no surface structure on the ridge waveguide. This demonstrates that this layer's ability to protect MgO:CLN from sputtering damage for device application. The domain structure in Fig. 9(b) has a pitch size of 600nm and a duty ratio of 35%, which is well consistent with the initial design. The sputtering depth in the protection layer is about 100nm (not shown in this paper), which is less than its initial thickness. This ensures the ridge waveguide to confine the propagating optical beam from

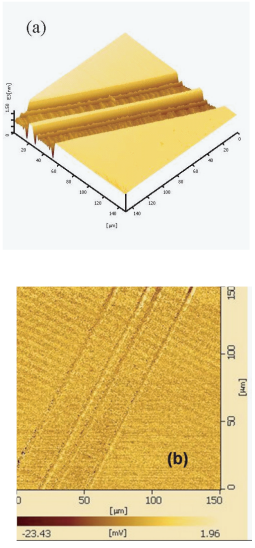

Fig. 8 Domain engineering in Mgo:CLN without resist coating. AFM image (a)and Piezoelectric force image (b).

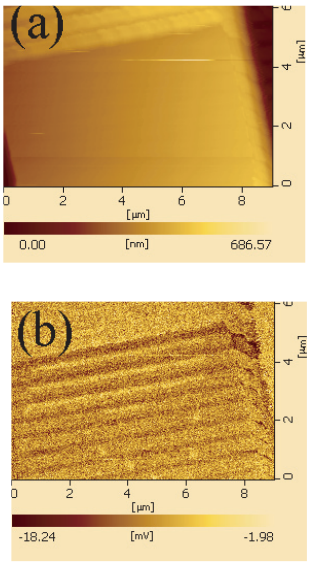

Fig.9 Domain engineering a MgO: CLNridge waveguide with resist coating. Surface morphology by AFM (left) and domain structure by PFM (right).

diffraction by the impact damage.

One of the drawbacks of FIB domain engineering is the small size of beam steering. Our present FIB system has a fabrication size of 200μm only. In order to fabricate a practical device, domain structure of several mm long is desired.

A home-design optical characterization system has been applied to study this device. The laser of 1064nm YAG laser was compressed to a beam of diameter of 100μm through lenses. This compressed beam has a pulse train of 30ns width and 10KHz repetition. Average power is around 300 mW. The pulse trains were directly focused into the small ridge waveguide by optimizing the device position with the largest green output. The sample was set in a Peltier thermostat. The green emission from the sample is illustrated by Fig. 10(a). The measured temperature dependence of the green output of the device is shown in Fig. 10 (b). It is clear that the green output has a temperature maximum at 34 centigrade, which is consistent with the working temperature design of the QPM device.

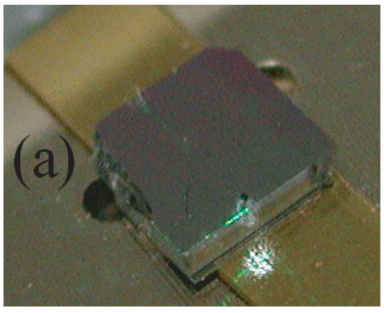

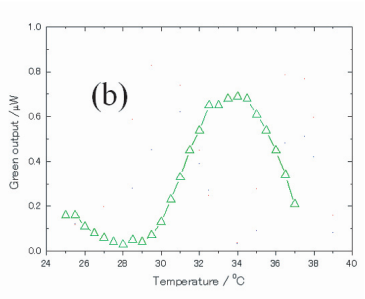

Fig. 10 Photograph of the green emission from the SHG device (a) and Temperature dependence of the SHG output (b).

The background outside of the sample was subtracted for estimating the device efficiency, which is estimated to be from 0.2 to 0.7%. The efficiency is very low due to the short device fabricated in this study. The device size is limited to 200 μ m due to the FIB facility. If a much fine sample stage movement controller, say with an accuracy of 100nm,is installed much longer device can be fabricated by repeated domain engineering with stage movement. Devices with much higher efficiency can be expected. The temperature dependence of the green output denonstrated is also a direct evidence of QPM.

5. Conclusion

We have exploited focused ion beam facility to nanofabricating lithium niobate for novel photonic devices and photonic integration. We exploited the domain fabrication ability of FIB in addition to its milling functions. Additionally, we optimize the best photonic crystal fabrication method that improves the photonic-crystal milling rate more than 20 times. Future demonstration of integrated photonic crystal based integrated nonlinear and EO devices are still under study.

References

(1) S. L. Lin et al., Nature, 394, 253 (1998).
(2) A. Sakai, G. Hara and T. Baba, Jpn. J. Appl. Phys. 40, L383-385 (2001).
(3) J. Kilby, Texas Instruments, 1958.
(4) R. Ulrich and H. P. Nolting, Integrated Optics (Springer-Verlag, Berlin, 1985)
(5) W. Barnes, A. Dereuxand T. Ebbesen, Nature 424, 824-830 (2003).
(6) J. D. Joannopoulos, R. D. Meade, and J. N. Winn, Photonic Crystal: Molding the flow of light (Princeton University Press, Princeton, 1995).
(7) B. Song, T. Asano, and S. Noda, J. Phys. D: Appl. Phys. 40, 2629-2634 (2007).
(8) J. O'Brien et al., J. Phys. D: Appl. Phys. 40, 2671-2682(2007).
(9) S. Fan et al., Phys. Rev. Lett. 80, 960 (1996).
(10) J. Yonekura, M. Ikeda, and T. Baba, J. Lightwave Technol. 17, 1500 (1999).
(11) S. Noda, A. Churinan and M. Imada, Nature 407, 408 (2000).
(12) H. Rong, R. Jones, A. Liu, O. Cohen, D. Hak, A. Fang and M. Paniccia, Nature 433, 725-728 (2005).
(13) Q. Xu, B. Schmidt, S. Pradhan and M. Lipson, Nature 435, 325-327 (2005).

(14) http://www.yamajuceramics.co.jp/english/product/top.html
(15) T. Baba and D. Mori, J. Phys. D: Appl. Phys. 40, 2659(2007).
(16) E. Ozbay, K. Aydin, I. Bulu and K. Geven, J. Phys. D: Appl. Phys. 40, 2652-2658 (2007).
(17) F. Lacour, N. Courjal, M.-P. Bernal, A. Sabac, C. Bainier and M. Spajer, Optical Materials 27, 1421 (2005).
(18) F. Lacour, N. Courjal, M.-P. Bernal, A. Sabac, C. Bainier and M. Spajer,, Appl. Phys. Lett. 87, 241101 (2005).
(19) Y. Y. Zhu and N. M. Ming, Optical and Quantum Electronics, 31, 1093 (1999).
(20) S. Miyazawa, J. Appl. Phys. 50, 4599 (1979).
(21) G. D. Miller, R. G. Batchko, M. M. Fejer, and R. L. Byer, Proc. SPIE 2700, 34 (1996).
(22) W. Hsu and M. C. Gupta, Appl. Phys. Lett. 60, 1 (1992).
(23) K. Mizuuchi et al., Opt. Lett. 28, 1344 (2003).
(24) X. Li, K. Terabe, H. Hatano, and K. Kitamura, Jpn. J. Appl. Phys. 51, L1550 (2005).
(25) X. Li, K. Terabe, H. Hatano, and K. Kitamura, JTuD-50, CLEO, Long Beach, 2006.
(26) X. Li, K. Terabe, H. Hatano, H. Zeng and K. Kitamura, J. Appl. Phys.100, 106103 (2006).
(27) X. Li, A. Watanabe, K. Terabe, H. Hatano, and K. Kitamura, CFN-6, CLEO, Baltimore, 2007.

筆 者 紹 介

李 西軍（リ シジュン）
技術開発本部 総合研究所 デバイス研究センター。高機能デバイス研究部第一研究室。強誘電ナノドメインの開発に従事。

渡 辺 温（ワタナベ アツシ）
技術開発本部 総合研究所 デバイス研究センター。高機能デバイス研究部。 DAT 用磁気ヘッド，青色半導体レーザの開発を経て，現在は強誘電ナノドメインの開発等に従事。